A Controlled NO-Releasing Compound: Synthesis, Molecular Structure, Spectroscopy, Electrochemistry, and Chemical Reactivity of *R,R,S,S-trans*-[RuCl(NO)(cyclam)]$^{2+}$(1,4,8,11-tetraazacyclotetradecane)

D. R. Lang,[†] J. A. Davis,[†] L. G. F. Lopes,[†] A. A. Ferro,[‡] L. C. G. Vasconcellos,[§] D. W. Franco,[§] E. Tfouni,*[,‡] A. Wieraszko,[||] and M. J. Clarke*[,†]

Merkert Chemistry Center, Boston College, Chestnut Hill, Massachusetts 02167, Departamento de Química, FFCLRP, Universidade de Sao Paulo, Ribeirão Preto, 14040-901, São Paulo, Brazil, Instituto de Química de São Carlos, Universidade de São Paulo, São Carlos, SP, Brazil, and Department of Biology, CUNY College of Staten Island, Staten Island, New York, 10314

Received November 8, 1999

The synthesis of *trans*-[RuCl(NO)(cyclam)]$^{2+}$ (cyclam = 1,4,8,11-tetraazacyclotetradecane) can be accomplished by either the addition of cyclam to $K_2[RuCl_5NO]$ or by the addition of NO to *trans*-[RuCl(CF_3SO_3)(cyclam)](CF_3SO_3). Crystals of *trans*-[RuCl(NO)(cyclam)](ClO_4)$_2$ form in the monoclinic space group $P2_1/c$, with unit cell parameters of $a = 7.66500(2)$ Å, $b = 24.7244(1)$ Å, $c = 16.2871(2)$ Å, $\beta = 95.2550(10)°$, and $Z = 4$. One of the two independent molecules in the unit cell lies disordered on a center of symmetry. For the ion in the general position, the Ru−N and N−O bond distances and the [Ru−N−O]$^{3+}$ bond angle are 1.747(4) Å, 1.128(5) Å, 178.0(4)°, respectively. In both ions, cyclam adopts the (R,R,S,S) configuration, which is also consistent with 2D COSY ^{1}H NMR studies in aqueous solution. Reduction ($E° = -0.1$ V) results in the rapid loss of Cl^- by first-order kinetics with $k = 1.5$ s^{-1} and the slower loss of NO ($k = 6.10 \times 10^{-4}$ s^{-1}, $\Delta H^{\ddagger} = 15.3$ kcal mol^{-1}, $\Delta S^{\ddagger} = -21.8$ cal mol^{-1} K^{-1}). The slow release of NO following reduction causes *trans*-[RuCl(NO)(cyclam)]$^{2+}$ to be a promising controlled-release NO prodrug for vasodilation and other purposes. Unlike the related complex *trans*-[Ru(NO)(NH_3)$_4$(P(OEt)$_3$)](PF_6)$_2$, *trans*-[RuCl(NO)(cyclam)]Cl_2 is inactive in modulating evoked potentials recorded from mice hippocampal slices probably because of the slower dissociation of NO following reduction.

Introduction

The ability of transition metal ions to both scavenge and release nitric oxide has generated a new interest in nitrosyl complexes as metallopharmaceuticals.[1] Nitroprusside, whose biological activity depends on the release of NO following reduction, has long been used as a powerful antihypertensive agent but is photosensitive and releases cyanide in vivo.[2,3] Effective scavengers of NO, such as [Ru^{III}(EDTA)(H_2O)], may be useful in treating toxic shock syndrome in which white blood cells generate a dangerously high level of NO in the bloodstream.[4,5]

Since the controlled release of NO from metallopharmaceuticals could be beneficial in a number of biomedical applications by affecting NO levels at specific sites, it is important to both modulate the rate of nitric oxide dissociation and prevent the occurrence of side reactions involving the metal. One way of doing this is to use macrocyclic ligands, which can provide an extremely stable, sequestered metal core, while also altering the metal ion's reactivity. For example, dielectric and solvation effects cause the affinity of chloride for Ru^{II} to increase between the complexes [Ru^{II}(NH_3)$_5$(H_2O)]$^{2+}$ ($K = 1.6$) and *trans*-[Ru^{II}(H_2O)$_2$(cyclam)]$^{2+}$ ($K = 32$).[6] Cyclam also restricts the pathways of other ligands to and from the axial coordination sites. Chloride is more rapidly lost from [Ru^{II}Cl(NH_3)$_5$]$^+$ ($k = 5$ s^{-1}) than from *trans*-[Ru^{II}Cl$_2$(cyclam)] ($k = 2.1 \times 10^{-2}$ s^{-1}), and loss of the second chloride occurs even more slowly.[7] Similarly, in a series of complexes of the type *trans*-[Ru^{II}Cl(cyclam)(py−X)]$^+$, where py−X = pyridine derivatives, py−X loss occurs both thermally and photochemically without observable chloride loss.[8]

We now report on the synthesis and characterization of complexes of the type *trans*-[Ru^{II}X(NO)(cyclam)]$^{2+}$, where X = halo or hydroxo ligand, and relate their biological effects to their chemical reactivities.

Experimental Section

Materials and Methods. All manipulations were carried out under inert atmosphere (N_2 or Ar) following conventional techniques. Milli-Q grade or doubly distilled water was used. $K_2[RuCl_5NO]$ was either obtained from Alfa Aesar or synthesized by a published method.[9]

[†] Boston College.
[‡] Departamento de Química, Universidade de Sao Paulo.
[§] Instituto de Química de São Carlos, Universidade de São Paulo.
[||] CUNY College of Staten Island.

(1) Clarke, M. J.; Gaul, J. B. *Struct. Bonding* **1993**, *81*, 147−180.
(2) Arnold, W. P.; Longnecker, D. E.; Epstein, R. M. *Anesthesiology* **1984**, *61*, 254−260.
(3) Shafer, P. R.; Wilcox, D. E.; Kruszyna, H.; Kruszyna, R.; Smith, R. P. *Toxicol. Appl. Pharmacol.* **1989**, *99*, 1−10.
(4) Fricker, S. P.; Slade, E.; Powell, N. A.; Vaughan, O. J.; Henderson, G. R.; Murrer, B. A.; Megson, I. L.; Bisland, S. K.; Flitney, F. W. *Br. J. Pharmacol.* **1997**, *122*, 1441−1449.
(5) Chen, Y.; Lin, F.-T.; Shepherd, R. E. *Inorg. Chem.* **1999**, *38*, 973−983.
(6) Walker, D. D.; Taube, H. *Inorg. Chem.* **1981**, *20*, 2828−2834.
(7) Poon, C. K.; Kan, Y. P.; Che, C. M. *J. Chem. Soc., Dalton Trans.* **1980**, 128−133.
(8) (a) Silva, M.; Tfouni, E. *Inorg. Chem.* **1997**, *36*, 274−277. (b) Silva, R. S.; Tfouni, E. *Inorg. Chem.* **1992**, *31*, 3313−3316.
(9) Durig, J. R.; McAllister, W. A.; Willis, J. N.; Mercer, E. E. *Spectrochim. Acta* **1966**, *22*, 1091−1100.

10.1021/ic9912979 CCC: $19.00
Published on Web 05/03/2000

Cyclam (1,4,8,11-tetraazacyclotetradecane) was obtained from Aldrich. When necessary, cyclam was recrystallized from chlorobenzene.

***trans*-[$RuCl_2$(cyclam)]Cl** was prepared by a slight modification of a previously described procedure.[6] An amount of 4.0 g (19 mmol) of $RuCl_3 \cdot 3H_2O$ was dissolved in 800 mL of ethanol in a three-necked flask. Hydrogen gas was bubbled through the solution for 2 h with continuous stirring followed by air-bubbling for another 2 h before adding 4.0 g (20 mmol) of cyclam to the solution and allowing the mixture to reflux for 14 h. Upon cooling to room temperature, the solution was filtered and the solvent was removed by rotary evaporation under reduced pressure. The resulting solid was dissolved in distilled water and loaded onto a cation-exchange resin (Dowex 50W-X2, 200−400 mesh), which was eluted with 0.1−1.0 M HCl. The fraction that eluted with 1 M HCl was collected and rotary-evaporated under reduced pressure to yield an orange solid, which was recrystallized from 1.0 M HCl. Yield: 53%.

***trans*-[RuCl(tfms)(cyclam)](tfms)** (tfms = trifluoromethanesulfonate) was prepared by dissolving 0.5 g (1.2 mmol) of *trans*-[$RuCl_2$(cyclam)]-Cl in 3.0 mL of trifluoromethanesulfonic acid (Htfms), CF_3SO_3H, under argon atmosphere in a three-necked flask. The solution was heated to 100 °C for 2 h. After cooling to room temperature, 50 mL of diethyl ether was added with vigorous stirring to induce the precipitation of a dark-green solid, which was collected by filtration, washed with diethyl ether, and stored in the dark under vacuum. Yield: 65%.

***trans*-[RuCl(NO)(cyclam)]$Cl_2 \cdot x H_2O$ (Method 1).** Equimolar amounts of cyclam (1.0642 g) and $K_2[RuCl_5NO]$ (1.9904 g) were refluxed in 300 mL of methanol for 36 h. After filtration of the reaction mixture through a glass frit, the filtrate was rotary-evaporated to dryness. The resulting brown residue was dissolved in water and loaded onto a Sephadex SP-C-25 cation exchange column 15 cm in height. A bluish band that eluted with water was discarded. The yellow product band eluted with 0.2 M HCl. This fraction was vacuum-rotary-evaporated to dryness, and the yellow residue was dissolved in 2:2:1 methanol/acetone/water solution before it was placed in an ether diffusion chamber for crystallization. Yellow needlelike crystals began to grow within a day. After 1 week, the crystals were collected by filtration and washed with ether and ethanol. All crystals, which were examined under a polarized-light microscope, were twinned. Yield: 40%. Variable amounts of water were found in the microanalytical results. This compound and related compounds with halide anions were soluble in water, methanol, and acetonitrile and were partially soluble in ethanol. Anal. Calcd for $4H_2O$ for $C_{10}H_{24}N_5Cl_3ORu$: C, 23.56; H, 6.33; N, 13.74; Cl, 20.86. Found: C, 23.77; H, 6.41; N, 13.82; Cl, 20.70. UV−vis (λ_{max}, nm (ϵ, M^{-1} cm^{-1})): 263 (3011), 334 (40), 433 (12.5), 456 (10). IR, cm^{-1}: 1869 (ν_{NO}). Electrochemistry (mV vs NHE by using $[(NH_3)_6Ru]^{3+/2+}$ as an internal standard in 0.1 M LiCl): $E^\circ_1 = -0.10$ V (irreversible), $E^\circ_2 = -0.15$ V (pH 2, reversible, pH-dependent).

***trans*-[RuCl(NO)(cyclam)]$(PF_6)_2$ (Method 2).** *Trans*-[Cl(CF_3SO_3)-(cyclam)Ru](CF_3SO_3) (0.5 g; 0.78 mmol) was dissolved in 50 mL of deaerated water. Nitric oxide, which was generated by dripping concentrated sulfuric acid onto $NaNO_2$ and passing it through a saturated aqueous solution of NaOH, was bubbled through the solution, causing the dark-green solution to slowly change to a light-yellow. After 3 h, 1 mL of a saturated aqueous solution of NH_4PF_6 was added and the mixture was left in the refrigerator for 6 h. The resulting yellow precipitate was collected by filtration and washed with diethyl ether and stored under vacuum in the dark. Anal. Calcd for $C_{10}H_{24}N_5$-$OClP_2F_{12}Ru$: C, 18.29; H, 3.68; N, 10.66; Ru, 15.39. Found: C, 18.20; H, 3.45; N, 10.32; Ru, 15.19. UV−vis (λ_{max}, nm (ϵ, M^{-1} cm^{-1})): 262 (2.5×10^3), 352 (1.9×10^2), 435 (54). IR, cm^{-1}: 1875 cm^{-1} (ν_{NO}). Electrochemistry: (0.1 M LiCl) −300 mV vs Ag/AgCl; (acetonitrile) $E^\circ_1 = -175$ mV (reversible, vs Ag/AgCl).

***trans*-[RuCl(NO)(cyclam)]$Br_2 \cdot x H_2O$** The bromide salt was prepared according to method 1 except that the column was treated with 3 M HBr beforehand and that the product was eluted with 0.2 M HBr. The product was crystallized from a 2:2:1 2-propanol/methanol/water solution in an ether diffusion chamber. All crystals were twinned. Yield: 40%. Anal. Calcd for $0.5H_2O$ for $C_{10}H_{24}N_5Cl_1Br_2O_1Ru$: C, 22.42; H, 4.70; N, 13.07; Cl, 6.62; Br, 29.83. Found: C, 22.26; H, 4.78; N, 12.94; Cl, 6.69; Br, 30.13. IR (cm^{-1}): 1852 (ν_{NO}).

***trans*-[RuCl(NO)(cyclam)]$(ClO_4)_2$.** *Caution*! Perchlorate salts may be explosive. *trans*-[RuCl(NO)(cyclam)]Cl_2 was dissolved in a minimum of water. An excess of a saturated aqueous $NaClO_4$ solution was added with an immediate formation of a yellow precipitate. The solid was filtered by vacuum filtration and washed with absolute ethanol. The product was recrystallized first from boiling H_2O, then hot 3 M $HClO_4$. The resulting crystals were collected and washed with ethanol. The compound was slightly soluble in hot water and acetonitrile. The crystals turned opaque on drying because of loss of solvent of recrystallization. Anal. Calcd for $C_{10}H_{24}N_5Cl_3O_9Ru$: C, 21.23; H, 4.28; N, 12.38; Cl, 18.80. Found: C, 22.17; H, 4.38; N, 12.39; Cl, 18.25. Attempts to prepare other salts by using $NaBPH_4$, NH_4PF_6, and NH_4I to provide other counterions resulted in products of varying purity.

Elemental Analyses. Analyses were performed by Robertson Microanalytical Laboratories or by the microanalytical laboratory of the Universidade de São Paulo, Instituto de Química.

Spectroscopy. UV−vis spectra were recorded on a Cary 2400 spectrophotometer in H_2O and also on a Hewlett-Packard 8452A diode array spectrophotometer. ^1H NMR spectra were obtained in 5 mm NMR tubes on Varian Unity 400 and 500 MHz FT spectrometers in D_2O (unless otherwise noted). IR spectra were obtained in KBr pellets and/or Nujol mulls on a Bomen MB-102, Nicolet 210, Nicolet 510 FT-IR, or Hewlett-Packard 5890 FTIR spectrophotometer.

Electrochemistry. Some electrochemical measurements were performed on millimolar solutions of the complexes in 0.1 M LiCl, 0.1 M $LiClO_4$, or 0.1 M $CF_3COOH/NaCF_3COO$ on a BAS 100a instrument. Reduction processes were first examined by cyclic voltammetry to ascertain the reversibility of each couple and then measured by square wave voltammetry from peak positions relative to an internal standard, $[Ru(NH_3)_6]^{3+,2+}$ (57 mV versus NHE). The working electrode was a hanging mercury drop electrode, the reference electrode was Ag/AgCl, and the counter electrode was platinum wire. Other cyclic voltammetry experiments were performed with a model 173 or a model 273 potentiostat/galvanostat from Princeton Applied Research. A glassy carbon electrode was used as the working electrode, and a platinum wire was used as an auxiliary electrode. Ag/AgCl reference electrodes were used in aqueous and nonaqueous solutions. Electrochemical experiments were performed in different media as follows: pH = 2.13 ($HNO_3/NaNO_3$, μ = 0.2 M); pH = 2.74 (potassium phthalate/HCl, μ = 0.2 M); pH = 3.93 (potassium phthalate/HCl, μ = 0.2 M); pH = 4.32 ($CF_3COOH/NaCF_3COO$, μ = 0.2 M); pH = 5.17 ($CF_3COOH/NaCF_3COO$, μ = 0.2 M); pH = 5.94 ($NaH_2PO_4 \cdot H_2O/Na_2HPO_4$, μ = 0.2 M); pH = 7.08 ($NaH_2PO_4 \cdot H_2O/Na_2HPO_4$, μ = 0.2 M); pH = 7.96 ($NaH_2PO_4 \cdot H_2O/Na_2HPO_4$, μ = 0.2 M); pH = 9.40 ($Na_2BO_4 \cdot 10H_2O/NaNO_3$, μ = 0.2 M); and in acetonitrile, μ = 0.20 M; tetrabutylammonium chloride. Potential values in the Results are usually given as the experimental data vs Ag/AgCl but are converted to values relative to NHE in the Discussion, where their biological significance is interpreted.

Kinetics. The first-order rate constant for the dissociation of Cl^- following the reduction of *trans*-[RuCl(NO)(cyclam)]Cl_2 was estimated from cyclic[10] and square wave voltammetric data obtained in 0.1 M $LiClO_4$ at 8 °C. Anodic scans were initiated from −0.9 V immediately after activating the cell. Data at scan rates of 0.1, 0.2, 0.5, 0.59, 0.8, and 1.5 V/s were digitally simulated for an ECE mechanism. The calculation was coupled to the nonlinear least-squares Solver function in Microsoft Excel to minimize the squared difference between the experimental and simulated reactant/product current peak ratios.

The loss of NO following the reduction of *trans*-[RuCl(NO)-(cyclam)]$^{2+}$ by Eu^{2+} was monitored by following the absorbance changes at 330 nm under argon. First-order rate constants (k_{obs}) were determined from the slope of $-\ln(A_\infty - A_t)$ versus time as determined by a standard linear least-squares method. Temperature was controlled to within ±0.2 °C. IR spectra were obtained on KBr pellets in air immediately following reduction of the compound with a drop of 0.02 M Eu^{2+} solution.

Crystallography. Initial crystal evaluation and data collection were performed on a Siemens SMART[11] system equipped with a CCD area detector and sealed-tube monochromated Mo Kα radiation. A large,

(10) Nicholson, R. S.; Shain, I. *Anal. Chem.* **1964**, *36*, 706.

Table 1. Crystal Data and Structure Refinement for *trans*-[RuCl(NO)(cyclam)]$(ClO_4)_2$

empirical formula	$C_{10}H_{20}Cl_3N_5O_9Ru$
fw	481.5
temp, K	203(2)
wavelength, Å	0.71073
space group	$P2_1/c$ (No. 14)
cryst syst	monoclinic
a, Å	7.665
b, Å	24.72440(10)
c, Å	16.2871(2)
β, deg	95.2550(10)
vol, Å^3	3073.48(4)
Z	4
density (calcd), g/cm^3	1.821
final R indices [$I > 2\sigma(I)$]	$R_1 = 0.0575$, $wR_2 = 0.1468$

orange twinned crystal of *trans*-[RuCl(NO)(cyclam)]$(ClO_4)_2$ was selected and cleaved to obtain an apparently single crystal. This was mounted on a thin glass fiber on a goniometer head using an epoxy resin and placed under a stream of nitrogen gas kept at −100 °C. An initial set of 60 frames with an exposure time of 10 s yielded a total of 216 reflections that were used to calculate orientation matrices and the preliminary cell constants. Three sets of frames of data were collected with 0.30° steps in ω and an exposure time of 10 s within a randomly oriented region of reciprocal space surveyed to the extent of 1.3 hemispheres to a resolution of 0.85 Å. By use of the program SAINT for the integration of the data,[12] reflection profiles were fitted and values of F^2 and $\sigma(F^2)$ for each reflection were obtained. Data were corrected for Lorentz and polarization effects. Averaging of equivalent reflections ($R_{merge} = 11.65\%$) yielded 7049 unique reflections with $I > 2\sigma(I)$. No semiempirical or decay correction was required. The space group $P2_1/c$ was chosen and confirmed by the successful refinement of the structure. The subroutine XPREP in SHELXTL[13] was used for the processing of data. Positions of most of the non-hydrogen atoms were obtained from a direct methods solution.[13] Several full-matrix least-squares and difference Fourier cycles were performed to locate the remainder of the non-hydrogen atoms. All non-hydrogen atoms were refined with anisotropic displacement parameters. All hydrogen atoms were placed in ideal positions and refined as riding atoms with individual isotropic displacement parameters. Crystallographic data are reported in Tables 1 and S1 (Table S1 in Supporting Information). The final positional and thermal parameters of the non-hydrogen atoms are listed in Table S2 of Supporting Information.

Effects on Hippocampal-Evoked Potentials. Brain slices were prepared from hippocampi of male (B6) mice as described elsewhere.[14] Animals were decapitated and the hippocampi removed from the brain and sectioned using a manual tissue slicer. The buffer composition (mM) was the following: NaCl, 124; KCI, 3; KH_2PO_4, 1.2; $MgSO_4$, 1.3; $CaCl_2$, 2.4; $NaHCO_3$, 26; glucose, 10.0 (33 °C, pH 7.4, aerated with 95% O_2/5% CO_2). Slices were positioned on a porous net in an "interface chamber" ($V = 1.2$ mL) in which the bottom of the slice was immersed in the oxygenated buffer. Hippocampal extracellular field potentials and population spikes were recorded from the pyramidal cell layer of the CA1 region. Slices were stimulated with bipolar electrodes placed on the Schaffer collaterals. A pulse stimulus at a current of 0.01−0.05 mA was applied for a duration of 150 μs at intervals of 30 s.[14] The response was quantified by measuring (A) the rate of rise of the excitatory postsynaptic potential (EPSP) and (B) the height of the population spike. The EPSP response was recorded from the dendritic region and reflects the current generated by the excitatory synaptic events.[15,16] Changes in the EPSP represent alterations in the potency of the synapses being activated.[16,17] The population spike represents the summated firing of CA1 pyramidal neurons. Changes in the population spike demonstrate alterations in neuron excitability.

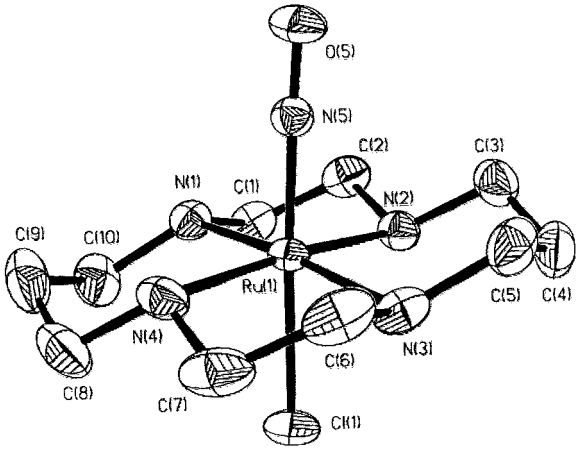

Figure 1. ORTEP Structure of *R,R,S,S-trans*-[RuCl(NO)(cyclam)]$^{2+}$. This ion is in a general position in the crystal.

Table 2. Bond Lengths around the Ruthenium Atom for *trans*-[RuCl(NO)(cyclam)]$(ClO_4)_2$

bond	bond distance (Å)	bond	bond distance (Å)
Ru(1)−Cl(1)	2.327(1)	N(5)−O(5)	1.128(5)
Ru(1)−N(1)	2.097(4)	Ru(2)−Cl(2)	2.318(5)
Ru(1)−N(2)	2.088(4)	Ru(2)−N(6)	2.081(5)
Ru(1)−N(3)	2.089(4)	Ru(2)−N(7)	2.092(4)
Ru(1)−N(4)	2.093(4)	Ru(2)−N(8)	1.73(3)
Ru(1)−N(5)	1.747(4)		

Results

Structure. An ORTEP diagram of the ruthenium ion, which was located in a general position in *trans*-[RuCl(NO)(cyclam)]-$(ClO_4)_2$, is shown in Figure 1. The second molecule sits on an inversion center and exhibits disorder between the NO and Cl moieties (see Figure S1 of Supporting Information). Bond lengths around the ruthenium atoms are given in Table 2. The bond distances and angles are statistically identical between the two molecules within 3σ; however, the disorder in the molecule on the inversion center led to slightly larger estimated standard deviations for this molecule and contributed to higher residuals for the overall structure. Both molecules are in the (R,R,S,S) configuration, which was also the minimum energy configuration given by MM2 calculations (see Figure 2).[18] The four amine nitrogens in Figure 1 are planar within a standard deviation of 0.0038 Å, and the Ru is displaced by 0.098 Å out of this plane toward the nitrosyl. The Cl(1)−H(N) distance of 2.6 Å, where N = N(2) and N(3), is similar to the analogous distance of 2.7 Å in *trans*-[$RuCl_2$(cyclam)]Br.[6]

^{1}H NMR and 2D COSY spectra (see Figure 3) were used to determine the structure of *trans*-[RuCl(NO)(cyclam)]Cl_2 in solution, which is shown in Figure 2. While the analysis of the spectrum is straightforward, an apparent triplet at 3.52 ppm is actually two partially overlapping doublets whose chemical shifts differ by only about 0.05 ppm. Similarly, the complex multiplet at 2.72 ppm is two overlapping triplets, whose chemical shifts also differ by ~0.05 ppm. While the diamagnetic anisotropy of the nitrosyl ligand differentiates the faces of the

(11) *SMART, Siemens Molecular Analytical Research Tool*, version 4.A50; Siemens Analytical X-ray Instruments, Inc.: Madison, WI, 1995.
(12) *SAINT, Data Reduction Software for Single Crystal Diffraction with an Area Detector*; Siemens Analytical X-ray Instruments, Inc.: Madison, WI, 1995.
(13) *SHELXTL-PLUS*, version 5.0; Siemens Industrial Automation Inc., Analytical Instrumentation: Madison, WI, 1995.
(14) Wieraszko, A.; Clarke, M. J.; Lang, D. R.; Lopes, L.; Franco, D. W. *Life Sci.*, submitted.
(15) Lomo, T. *Exp. Brain Res.* **1971**, *12*, 18−45.
(16) Andersen, P.; Bliss, T. V. P.; Skrede, K. K. *Exp. Brain Res.* **1971**, *13*, 65−79.
(17) Andersen, P.; Holmquist, B.; Voorhoere, P. E. *Acta Physiol. Scand.* **1966**, *66*, 448−460.
(18) Allinger, N. L. *J. Am. Chem. Soc.* **1977**, *99*, 8127.

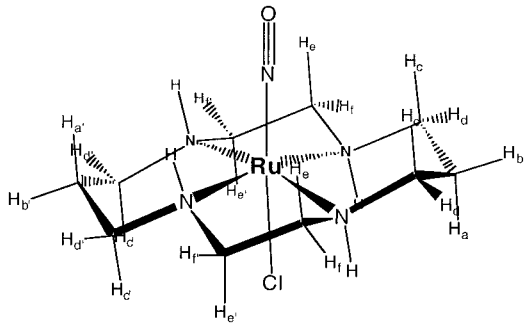

Figure 2. Solution structure of *R,R,S,S-trans*-[RuCl(NO)(cyclam)]Cl_2·$4H_2O$ from 2D COSY ^{1}H NMR studies. Structure shown was minimized by MM2 calculations.[18] Metal−ligand bond distances were held at the crystallographic values.

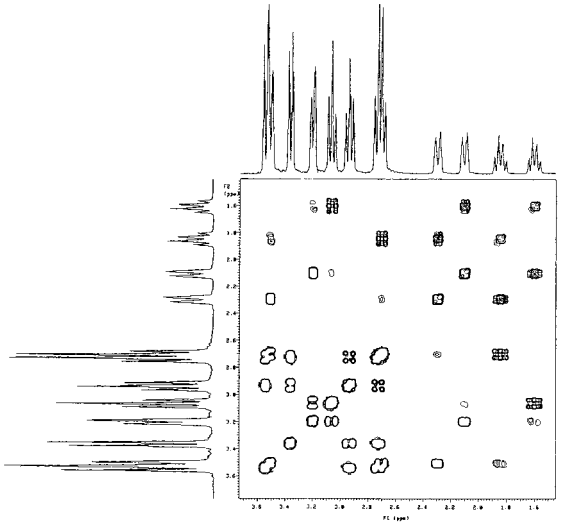

Figure 3. 2D-COSY spectrum of *trans*-[RuCl(NO)(cyclam)]Cl_2 in D_2O at 500 MHz.

Table 3. ^{1}H NMR Spectral Results for *trans*-[RuCl(NO)(cyclam)]Cl_2·$4H_2O$ in D_2O

assignment	chemical shift δ (ppm)
a, a′	1.60q, 1.86q
b, b′	2.12d, 2.30d
c, c′	3.08t, 2.72t
d, d′	3.22d, 3.52d
e, e′	2.72t, 2.95t
f, f′	3.52d, 3.38d

complex, calculations assuming only an axial magnetic field were insufficient to systematically distinguish between nearly symmetric hydrogens (see Figure 2 and Table 3).

Electrochemistry. The cyclic voltammetric scan of *trans*-[RuCl(NO)(cyclam)]$^{2+}$ (3 °C, 30 mV/s, 0.1 M NaF_3CCOO/HF_3CCO_2, pH 4.32) shown in Figure 4 exhibits three electrochemical processes (vs Ag/AgCl): Ep_{c1} at −0.320, Ep_{c2} at −0.470 V, and Ep_a at −0.360 V. Peak 2c is pH-dependent between pH 1.74 and 9.30, while the others are pH-independent. In 0.1 M LiCl at pH 5.8 (10 °C, 100 mV/s scan rate), only two electrochemical peaks were seen (Ep_{c1} at −0.370 V and Ep_{a1} at −0.220 V), while peak 2c was no longer observed. Since the ratio of the cathodic peak heights (ip_{c1}/ip_{a1}) approaches unity with increasing scan rate, the irreversibility of the E_1 process appears to be due to the loss of chloride following reduction to *trans*-[RuCl(NO$^\bullet$)(cyclam)]$^+$ (eq 2, Scheme 1).

A small bathochromic IR shift (22−30 cm^{-1}) in the nitrosyl IR stretching frequency was observed following reduction by Eu^{2+} in air.[19] Above pH 10, the E_1 couple disappears probably because of base-catalyzed loss of chloride to give *trans*-[Ru(OH)(cyclam)(NO)]$^{2+}$. Consequently, the chemically irreversible process, $E°_1$ in Scheme 1 (−0.10 V vs NHE), which is independent of pH between pH 4 and 10, is attributed to *trans*-[RuCl(NO)(cyclam)]$^{2+/+}$.

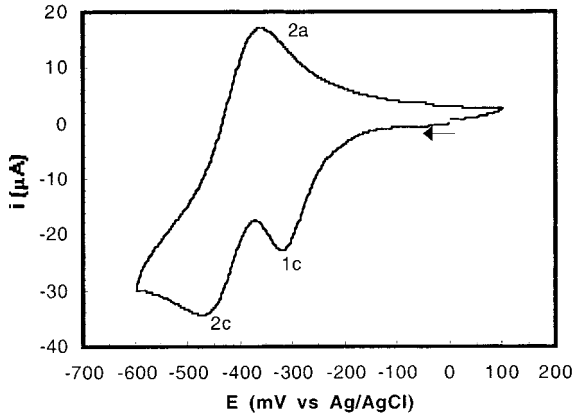

Figure 4. Cyclic voltammetric scan of *trans*-[RuCl(NO)(cyclam)]$(PF_6)_2$ at pH 4.32 ($CF_3COOH/NaCF_3COO$) at 30 mV/s and 3 °C.

Scheme 1

$$\textit{trans}\text{-}[RuCl(NO)(cyclam)]^{2+} + e^- \underset{k_1}{\overset{E_1}{\rightleftarrows}} \textit{trans}\text{-}[RuCl(cyclam)(NO^\bullet)]^+ \quad (1)$$

$$\textit{trans}\text{-}[RuCl(cyclam)(NO^\bullet)]^+ + H_2O \xrightarrow{k_2} \textit{trans}\text{-}[Ru(H_2O)(cyclam)(NO\cdot)]^{2+} + Cl^- \quad (2)$$

$$\textit{trans}\text{-}[Ru(H_2O)(cyclam)(NO^\bullet)]^{2+} + H_2O \xrightarrow{k_3} \textit{trans}\text{-}[(H_2O)_2(cyclam)Ru]^{2+} + NO^\bullet \quad (3)$$

$$\textit{trans}\text{-}[Ru(H_2O)(NO)(cyclam)]^{2+} + e^- \xrightarrow{E_2} \textit{trans}\text{-}[Ru(H_2O)(cyclam)(NO^\bullet)]^{2-} \quad (4)$$

$$\textit{trans}\text{-}[Ru(H_2O)(NO^\bullet)(cyclam)]^+ + e^- \xrightarrow{E_3} \textit{trans}\text{-}[Ru(H_2O)(cyclam)(NO^-)] \quad (5)$$

$$\textit{trans}\text{-}[Ru(H_2O)(cyclam)(NO^-)]^+ + H_2O \xrightarrow{k_4} \textit{trans}\text{-}[Ru(H_2O)_2(cyclam)]^{2+} + NO^- \quad (6)$$

$$\textit{trans}\text{-}[Ru(H_2O)_2(cyclam)]^{3+} + e^- \xrightarrow{E_4} \textit{trans}\text{-}[Ru(H_2O)_2(cyclam)]^{2+} \quad (7)$$

When estimated by cyclic and square wave voltammetric methods,[10,20] the first-order rate constant (k_2) for loss of the chloride following reduction was ∼1.5 s^{-1} at pH 4 in 0.1 M sodium acetate or sodium trifluouroacetate aqueous solutions.

The second electrochemical couple (E_2 in Scheme 1) was pH-dependent and is attributed to the reduction of [Ru^{II}(H_2O)(cyclam)(NO)]$^{3+}$ to [Ru^{II}(H_2O)(cyclam)(NO$^\bullet$)]$^{2+}$. A plot of Epc_2 versus pH yielded estimates of $pK_{a(ox)}$ and $pK_{a(red)}$ as 3.0 and 6.4, respectively, where $K_{a(ox)}$ is the ionization constant for the

(19) Schreiner, A. F.; Lin, S. W.; Hauser, P. J.; Hopcus, E. A.; Hamm, D. J.; Gunter, J. D. *Inorg. Chem.* **1972**, *11*, 880.
(20) Sawyer, D. T.; Roberts, J. L. *Experimental Electrochemistry for Chemists*; Wiles: New York, 1974.

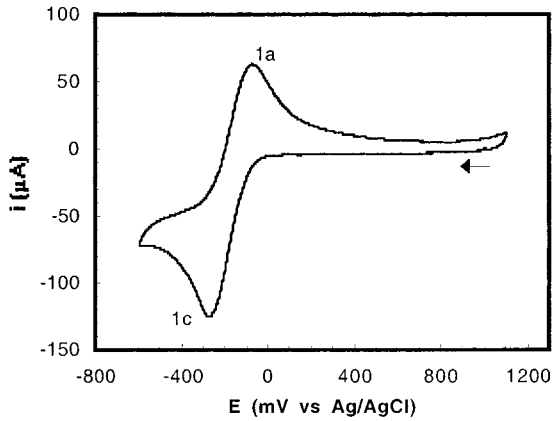

Figure 5. Cyclic voltammetry of *trans*-[RuCl(cyclam)NO]$^{2+}$ in acetonitrile: [Ru] = 5 × 10^{-4} M^{-1}; μ = 0.20 M^{-1} with tetrabutylammonium chloride; 25 °C; 100 mV s^{-1}; reference electrode = Ag/AgCl.

oxidized form and $K_{a(red)}$ is the ionization constant for the reduced form.

$$trans\text{-}[Ru^{II}(H_2O)(cyclam)(NO^{\bullet})]^{2+} \rightarrow trans\text{-}[Ru^{II}(HO^{-})(cyclam)(NO^{\bullet})]^{+} + H^{+} \qquad (pK_{a(ox)} \approx 3.0)$$

$$trans\text{-}[Ru^{II}(H_2O)(NO^{-})(cyclam)]^{+} \rightarrow trans\text{-}[Ru^{II}(HO^{-})(NO^{-})(cyclam)] + H^{+} \qquad (pK_{a(red)} \approx 6.4)$$

When electrochemical scans were extended below −1.4 V vs Ag/AgCl, an additional irreversible reduction process occurred at −1.18 V, which is attributed to the reduction of *trans*-[Ru^{II}(H$_2$O)(cyclam)(NO$^{\bullet}$)]$^{+}$ followed by loss of NO^{-} (eqs 5 and 6 in Scheme 1). At pH 4.32, a reversible couple was observed at −90 mV vs Ag/AgCl (E_4 in Scheme 1, 132 mV vs NHE),[20] which is similar to the reported $E°$ value (155 mV vs NHE, pH 1) for *trans*-[Ru(H$_2$O)$_2$(cyclam)]$^{2+/3+}$.[6]

In acetonitrile (25 °C, 100 mV s^{-1}, 0.1 M (*n*-Bu)$_4$ClO$_4$), the E_1 process (Ep$_{c1}$ = 0.262 V, Ep$_{a1}$ = −0.082 V vs Ag/AgCl) was observed over the potential range −1.1 to 1.1 V. A partially irreversible E_3 cathodic process was observed at −0.94 V.

EPR. Consistent with the stability of *trans*-[Ru(H$_2$O)(cyclam)(NO$^{\bullet}$)]$^{2+}$ evident in the electrochemical experiments, addition of Eu^{II} to an aqueous solution of *trans*-[RuCl(NO)(cyclam)]$^{2+}$ under strictly anaerobic conditions results in the appearance of an ESR signal (Figure 6) with g_x = 1.995, g_y = 2.035, g_z = 1.883, A_x = 32.1 G, A_y = 17 G, and A_z = 15 G. Taken together, the fine and nitrogen hyperfine structures are consistent with the unpaired electron being involved with a NO π^* orbital following reduction to yield an octahedral {M−NO}^{7} system with significant NO$^{\bullet}$ character.[21,22]

Dissociation of NO. Following bulk reduction of *trans*-[RuCl(NO)(cyclam)]$^{2+}$ with Eu^{2+}, changes in the UV−vis spectra are observed (Figure 7). At first, the absorbances at 260 and 350 nm decrease while a band at 330 nm appears. The 330 nm band then decreases with time. Addition of one drop of Eu^{2+} solution to a KBr pellet of *trans*-[RuCl(NO)(cyclam)]$^{2+}$ resulted in a small shift of the nitrosyl IR stretching frequency from 1875 to 1853 cm^{-1}. Schreiner has noted that the trans ligand has a slight effect on the ν(NO). In general, *trans*-chloride frequencies are ∼30 cm^{-1} higher than the corresponding *trans*-hydroxo compounds,[19] so the shift in the IR band from 1875 to 1853 cm^{-1} is consistent with substitution of the chloride by water or hydroxide;[19] however, shifts this small have been attributed to coordinated NO$^{\bullet}$.[23]

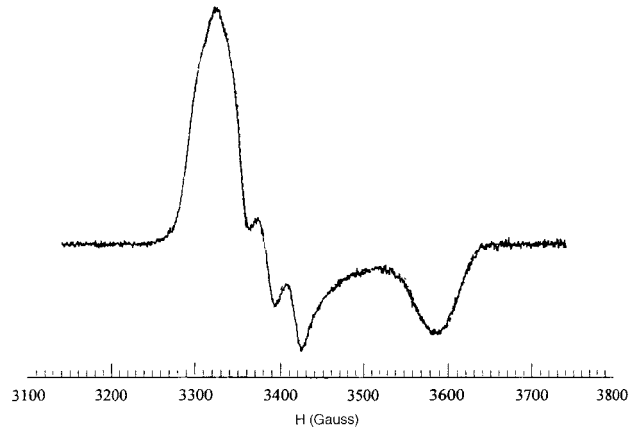

Figure 6. Powder ESR spectrum of *trans*-[Ru(H$_2$O)(NO·)(cyclam)]$^{2+}$ in glycerol/water (70:30) solution at 77 K following reduction of the coordinated NO^{+} in *trans*-[RuCl(NO)(cyclam)]$^{2+}$.

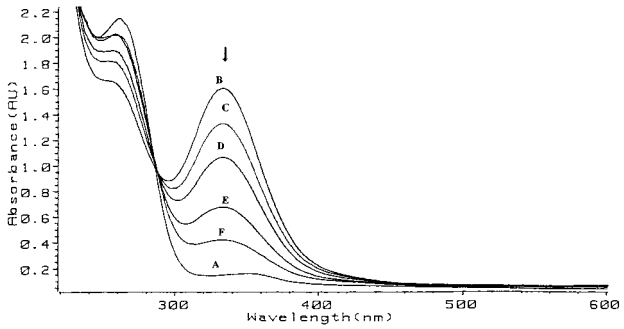

Figure 7. Sequence of electronic spectra showing the decrease of the absorption band assigned to the NO labilization: (A) *trans*-[RuCl(NO)(cyclam)]$^{2+}$; (B) *trans*-[Ru(H$_2$O)(cyclam)(NO$^{\bullet}$)]$^{2+}$.

The loss of NO following single-electron reduction by Eu^{2+} appears to proceed by the series of reactions indicated in Scheme 1, with the reducing electron provided by Eu^{2+}, where k_1, $k_2 \gg k_3$. The first-order rate constant for loss of NO$^{\bullet}$ from *trans*-[Ru(H$_2$O)(cyclam)(NO$^{\bullet}$)]$^{+}$, k_3, is 6.10 × 10^{-4} s^{-1} at 25 °C, with the following activation parameters: $\Delta H^{\ddagger}$ = 15.3 ± 0.3 kcal mol^{-1}, $\Delta S^{\ddagger}$ = −21.8 ± 0.3 cal mol^{-1} K^{-1}, and $\Delta G^{\ddagger}$ = 21.8 kcal mol^{-1} (Figure S3).

Since the $E°$ for the Eu$^{III/II}$ couple (−0.34 V vs NHE)[24] is less than E_{pc1} for the *trans*-[Ru(H$_2$O)(cyclam)(NO)]$^{2+}$, the loss of NO is attributed to *trans*-[Ru(H$_2$O)(cyclam)(NO$^{\bullet}$)]$^{+}$. Dissociation of nitric oxide after reduction with Eu^{2+} was also followed by monitoring a shift in the nitrosyl IR stretching frequency and by observing a loss of the EPR signal. When a frozen solution of *trans*-[RuCl(cyclam)(NO$^{\bullet}$)]$^{+}$, which was prepared by the reduction of *trans*-[RuCl(NO)(cyclam)](PF$_6$)$_2$ at pH 2 with 1 equiv of Eu^{2+} at 25 °C, frozen at 77 K, was quickly returned to room temperature and the EPR spectrum acquired after 5 half-lives for the loss of NO$^{\bullet}$, no signal was present.

Biological Testing. Screening of the compound *trans*-[RuCl(NO)(cyclam)]Cl$_2$ by the National Cancer Institute Developmental Therapeutics Program showed no significant anticancer

(21) Ferro, A. A.; Bezerra, C. W. B.; Battaglin, I.; Tfouni, E.; Franco, D. W.; McGarvey, B. Unpublished results, 1999.
(22) Chen, Y.; Sweetland, M. A.; Shepherd, R. E. *Inorg. Chim. Acta* **1997**, *260*, 163.
(23) Bagatin, I. A.; Toma, H. E. *Spectrosc. Lett.* **1996**, *29*, 1409−1416.
(24) Cotton, F. A.; Wilkinson, G.; Murillo, C. A.; Bochmann, M. *Advanced Inorganic Chemistry*, 5th ed.; Wiley-Interscience: New York, 1999.

activity in terms of toxicity against various cancer cell lines in tissue culture. No increase in the number or potential of neurons firing was evident for either *trans*-[RuCl(NO)(cyclam)]Cl_2·4H_2O or *trans*-[$RuCl_2$(cyclam)]Cl_2·2H_2O in screening for effects on electrochemical neuronal signals in the mouse hippocampus.[14] Results reported elsewhere reveal a relatively long-lasting antihypertensive effect in male Wistar rats.[25]

Discussion

Structure. The short Ru−NO and N−O distances together with the nearly linear Ru−N−O bond angle seen in *trans*-[RuCl(NO)(cyclam)]$^{2+}$ (Figure 1 and Table 2) are similar to the averages derived from nine other ruthenium nitrosyl structures of 1.75(3) Å, 1.19(3) Å, and 176(4)°, respectively,[26−35] and are close to those in *trans*-[RuCl(NO)(NH_3)$_4$]Cl_2 (1.79(1) Å, 1.08(2) Å, and 180(1)°, respectively)[36] and in *trans*-[Ru(NO)(NH_3)$_4$(H_2O)]Cl_3·H_2O (1.715(5) Å, 1.142(7) Å, 178.1(5)°, respectively).[35] The short Ru−N bond and nearly linear Ru−N−O bond angle are indicative of multiple bonding between the Ru and the nitrosyl, which can be indicative of the nitrosonium character in the nitrosyl. In the most closely related macrocyclic structure, *trans*-[Ru(OH)(NO)L](ClO_4)$_2$, where L = 1,5,9,13-tetramethyl-1,5,9,13- tetraazacyclohexadecane, the average Ru−NO and N−O bond lengths are 1.74(2) Å and 1.13(2) Å, respectively, and the average Ru−N−O bond angle is 176(3)°.[34] The average Ru−N_{cyclam} bond length of 2.092(4) Å (Table 2) is similar to 2.14(4) Å in *R,S,R,R-trans*-[Ru^{II}(N_3)(CH_3N)(1,4,8,-11-tetramethyl-14ane)]$^+$,[37] in which the steric bulk of the methyl groups results in a "three-up and one-down" configuration, and 2.083(3) Å in *R,R,S,S-trans*-[$Ru^{III}Cl_2$(cyclam)]Br, and 2.098 Å in *R,R,S,S-trans*-[RuCl(4-acpy)(cyclam)](BF_4),[38] in which the cyclam adopts the same configuration as reported here.

The disorder of the molecule on the inversion center may also admit the synthetic starting complex, *R,R,S,S-trans*-[Ru^{III}-Cl_2(cyclam)]$^+$, which may account for impurities and variable chloride analyses encountered in attempts to prepare related complexes. The slight displacement of Ru out of the plane of the amine nitrogens (0.098 Å) is similar to 0.126 Å, which occurs for *trans*-[RuCl(cyclam)(4-acpy)](BF_4).[38] As in *trans*-[$RuCl_2$(cyclam)]Br [6] and *trans*-[RuCl(cyclam)(4-acpy)](BF_4),[38] there appears to be significant hydrogen bonding, Cl(1)−H(N) (2.7 Å), which may stabilize the chloride. The short Cl(1)−H(N) distance may also be partly due to the nitrosyl's pulling of the Ru out of the plane of the cyclam ligand. Such a hydrogen-bonding interaction could account for the slight N(5)−Ru(1)−Cl(1) bond angle that displaces the Cl toward N(2) and N(3) (see Figure S2). The 2D NMR results indicate that the solid-state configuration of *trans*-[RuCl(NO)(cyclam)]$^{2+}$ is present in solution (Figures 1 and 2), as also occurs with the *trans*-[RuCl(cyclam)(4-acpy)](BF_4)[39] and *trans*-[$RuCl_2$(cyclam)]-Br.[6]

Spectra. Since *trans*-[RuCl(NO)(cyclam)]$^{2+}$ is structurally and electronically similar to the ruthenium tetraammine nitrosyls [L(NO)(NH_3)$_4$Ru]X_n (L = Cl^-, Br^-, NCO^-, N_3^-, OH^-, NH_3 or $CH_3CO_2^-$; X = Cl^-, Br^-, I^-, or ClO_4^-), it is likely that the UV−visible spectra are analogous.[19] In the compounds presented here, the UV−vis spectra are dominated by a relatively intense band in the 260−280 nm region, which is assigned to an LMCT charge-transfer band (π_p(Cl) → e_g(Ru)).[19] The peak at 334 nm is assigned to a spin-allowed d−d transition $^1A_1$ → $^1T_1$ but is significantly less intense than that in [Ru(NO)(NH_3)$_5$]$^{3+}$.[19] Broadening of this band can be attributed to tetragonal splitting of the $^1T_1$ excited state into $^1A_2$ and ^1E states. The two small peaks in the 430−460 nm region are characteristic of interconfigurational spin-forbidden transitions ($^1A_1$ → $^3T_1$ and $^1A_1$ → $^3T_2$) evident in 4d and 5d compounds, which may also have a t_{2g}(Ru) → π^*(NO) component. However, in *trans*-[Ru(NO)(NH_3)$_4$(H_2O)]$^{3+}$, the bands in this range appear to correspond to transitions involving molecular orbitals extending over Ru, H_2O, and NO.

The ν_{NO} for *trans*-[RuCl(NO)(cyclam)]$^{2+}$ (1875 cm^{-1}) is in the range generally associated with nitrosonium complexes[39] and is comparable to those of *trans*-[RuX(NO)(NH_3)$_4$]$^{2+}$, where X = Cl (1880 cm^{-1}), Br (1882 cm^{-1}), I (1884 cm^{-1}), CH_3O_2 (1882 cm^{-1}),[19] and OH (1834, 1858, and 1847 cm^{-1}).[19,26,41] It is red-shifted relative to those of *trans*-[Ru(NO)L(NH_3)$_4$]Cl_3, where L = NH_3 (1913, and 1953 cm^{-1})[26,41] and H_2O (1912 cm^{-1}),[35] which probably arises from relatively more electron donation from Cl^-, thereby slightly increasing the Ru^{II} → π^*_{NO} back-bonding.[35] The small bathochromic shift of ν_{NO} ($\Delta\nu$ = 22−30 cm^{-1}) following reduction of *trans*-[RuCl(NO)(cyclam)]$^{2+}$ by Eu^{2+} in acid in air is consistent with a redox−catalytic substitution of Cl^- by OH^- ($\Delta\nu$ = 22−46 cm^{-1}; see above),[19] but similar shifts have been attributed to $\nu(NO^{\bullet})$.[40]

Increasing nitrosyl stretching frequencies (ν_{NO} > 1886 cm^{-1}) generally correlate with the facility with which coordinated nitrosyl undergoes nucleophilic attack by OH^- to form NO_2^-.[36,41] Consequently, as with *trans*-[Ru(NO)(NH_3)$_4$(OH)]$^{2+}$ (ν_{NO} = 1858 cm^{-1}),[35] which has a similar degree of Ru^{II}−π^*_{NO} back-bonding, the conversion of NO to NO_2^- in *trans*-[RuCl(NO)-cyclam]$^{3+}$, ν_{NO} (1875 cm^{-1}), was not observed spectrophotometrically below pH 12.

Electrochemistry. Since ruthenium centers in nitrosyl complexes are not electroactive until about 1.4 V,[36,42,43] it is reasonable to assume that the first reduction process (peak 1c in Figure 4) occurs at the NO^+ (eq 1, Scheme 1) to yield coordinated $NO^{\bullet}$. At scan rates greater than 500 mV s^{-1}, the virtual disappearance of peaks 2a (−360 mV) and 2c (−470 mV) occurs in concert with the apparent reversibility of the

(25) Marcondes, F. G.; Souza-Torsoni, A.; Sumitami, M.; Franco, D. W.; Ferro, A. A.; Tfouni, E.; Krieger, M. H. Submitted for publication.
(26) Bottomley, F. J. *J. Chem. Soc., Dalton Trans.* **1974**, 1600−1605.
(27) Abraham, F.; Nowogrocki, G.; Sueur, S.; Bremard, C. *Acta Crystallogr., Sect. C: Cryst. Struct. Commun.* **1983**, *39*, 838.
(28) Pierpont, C. G.; Eisenberg, R. *Inorg. Chem.* **1972**, *11*, 1094.
(29) Pierpont, C. G.; Eisenberg, R. *Inorg. Chem.* **1972**, *11*, 1088.
(30) Pierpont, C. G.; Eisenberg, R. *Inorg. Chem.* **1973**, *12*, 199.
(31) Reed, J.; Schultz, A. J.; Pierpont, C. G.; Eisenberg, R. *Inorg. Chem.* **1973**, *12*, 2949.
(32) Hall, D.; Williamson, R. B. *Cryst. Struct. Commun.* **1974**, *3*, 327.
(33) Szczepura, L. F.; Muller, J. G.; Bessel, C. A.; See, R. F.; Janik, T. S.; Churchill, M. R.; Takeuchi, K. J. *Inorg. Chem.* **1992**, *31*, 859.
(34) Wong, K.-Y.; Mak, T. C. W.; Che, C.-M.; Yip, W.-H.; Wang, R.-J. *J. Chem. Soc., Dalton Trans.* **1992**, 1417−1421.
(35) Bezerra, C. W. B.; da Silva, S. C.; Gambardella, M. T. P.; Santos, R. H. A.; Plicas, L. M. A.; Tfouni, E.; Franco, D. W. *Inorg. Chem.* **1999**, *38*, 5660−5667.
(36) Bezerra, C. W. B. D.Sc. Thesis, Universidade de São Paulo, São Carlos, SP, Brazil, 1999.
(37) Che, C.-M.; Lai, T.-F.; Lau, K.; Mak, T. C. W. *J. Chem. Soc., Dalton Trans.* **1988**, 239−241.
(38) Silva, R. S.; Gambardella, M. T. P.; Santos, R. H. A.; Mann, B. E.; Tfouni, E. *Inorg. Chim. Acta* **1996**, *245*, 215−221.
(39) Richter-Addo, G. B.; Legzdins, P. *Metal Nitrosyls*; Oxford University Press: New York, 1992.
(40) Bagatin, I. A.; Toma, H. E. *Spectrosc. Lett.* **1996**, *29*, 1409−1416.
(41) Bottomley, F.; Brooks, W. V. F.; Clarkson, S. G.; Tong, S.-B. *J. Chem. Soc., Chem. Commun.* **1973**, 919−920.
(42) Gomes, M. G.; Davanzo, C. U.; Silva, S. C.; Lopes, L. G. F.; Santos, P. S.; Franco, D. W. *J. Chem. Soc., Dalton Trans.* **1998**, 601−607.
(43) Borges, S. S. S.; Davanzo, C. U.; Castellano, E. E.; Zukerman-Schpector, J.; Silva, S. C.; Franco, D. W. *Inorg. Chem.* **1998**, *37*, 2670−2677.

coupled peaks 1a (−250 mV) and 1c (−320 mV). The dependence of the CV peaks on the scan rate is similar to that observed with *trans*-$[RuCl(NO)(NH_3)_4]^{2+}$ and is consistent with the loss of chloride (eq 2, Scheme 1).[36] Peaks 2a and 2c, which are associated with the hydroxide complex, are suppressed in 0.10 M LiCl or in acetonitrile, where only the E_1 and E_3 electrochemical processes (Scheme 1) are observed. Consequently, the reduction potentials (vs Ag/AgCl) of *trans*-[RuCl(NO)cyclam]$^{2+/+}$ (CV peaks 1a and 1c) are assigned as −300 mV in 0.1 M LiCl and −175 mV in CH_3CN.

Relative to NHE, the $E°$ of −0.1 V for *trans*-[RuCl(NO)(14ane)]$^{2+}$ in aqueous solution is somewhat higher than might be expected on the basis of the reduction potential of $[Ru(NH_3)_5(NO)]^{3+}$ ($E° = -0.12$ V)[44] and *trans*-$[Ru(H_2O)(NH_3)_4(NO)]^{3+}$ ($E° = -0.15$ V) or the value estimated from Lever parameters (−0.16 V), but the small difference may be attributed to the lower dielectric medium provided by the macrocyclic ligand. Since the reduction potentials for the addition of the first and second electrons to the nitrosyl ligand typically differ by about 0.8 V,[1,45] the second reduction process (−0.15 mV vs NHE at pH 2) is considerably higher than expected for the reduction of $[RuCl(NO^{\bullet})(14ane)]^{+}$ to $[RuCl(NO^{-})(14ane)]$ but essentially identical to that of *trans*-$[Ru(H_2O)(NH_3)_4(NO)]^{3+}$. Because increasing scan rate causes the current peaks in the E_2 process to decrease relative to those in the E_1 process, the second reduction appears to involve the product of the initial EC reaction, i.e., the aqua/hydroxo species. Consequently, the second process is attributed to the pH-dependent reduction of $[Ru(H_2O)(14ane)(NO)]^{3+}$ to $[Ru(H_2O)(NO^{\bullet})(14ane)]^{2+}$. The p$K_a$ values of ∼3 and 6.5 for *trans*-$[Ru(H_2O)(cyclam)(NO)]^{3+}$ and *trans*-$[Ru^{II}(H_2O)(NO\cdot)(cyclam)]^{2+}$, respectively, are similar to those for *trans*-$[Ru(H_2O)(NO^{+})(NH_3)_4]^{3+}$ (3.1 ± 0.1) and *trans*-$[Ru(H_2O)(NO^{\bullet})(NH_3)_4]^{2+}$ (7.7 ± 0.1).[35] When run in 0.2 M $(Bu_4N)Cl$ in acetonitrile, where chloride dissociation was suppressed, the separation between E_1 and E_2 (*trans*-[RuCl(NO)(cyclam)]$^{+/0}$ is the expected 0.8 V.[1] In aqueous media, the irreversible cathodic process at about −1 V is attributed to the reduction of *trans*-$[Ru^{II}Cl(NO^{\bullet})(cyclam)]^{+}$ or, more likely, $[Ru(H_2O)(NO^{\bullet})(NH_3)_4]^{2+}$.

Biological Activity. While the reduction potential of *trans*-$[RuCl(NO)(cyclam)]Cl_2$ is biologically accessible, the resulting dissociation of NO is probably too slow to provide sufficient NO for the synaptic effect. This is in contrast to the high neurological activity observed with *trans*-$[(NO)((CH_3CH_2O)_3P)(NH_3)_4Ru]^{2+}$, in which the phosphito ligand exerts a strong trans effect to labilize the nitrosyl such that it is lost rapidly under physiological conditions.[46] The low cytotoxicty in the NCI anticancer screen may also arise from a rate of NO generation that is too low to significantly affect cells.

The inherently high stabilities of macrocyclic complexes coupled with the high affinity of ruthenium for nitric oxide may lead to better NO scavengers in combating detrimental effects of NO in vivo, such as vasodilation resulting from NO in toxic shock syndrome.[4,47] Since dissociation of NO from *trans*-[RuCl(NO)(cyclam)]$^{2+}$ ($k_{obs} = 6.1 \times 10^{-4}$ s^{-1}) is an order of magnitude slower than that of $[Ru(NO)(Hedta)]^{2+}$ ($k_{obs} = 7.3 \times 10^{-3}$ s^{-1}),[48] it may be a better NO binding agent. A potential advantage of *trans*-$[RuCl(H_2O)(cyclam)]^{2+}$ and related complexes is their low toxicity.[26,49]

Modulating the Ru−NO bond strength in Ru^{II} complexes by adjusting the π-acceptor strength of the opposing ligand should provide a way to precisely tune dissociation rates of the Ru−NO bond.[1,48] Related work in our laboratories reveals that the slow release of NO following reduction of the cyclam complex results in an immediate lowering of blood pressure. This effect persists 26 times longer than that of the of the clinically used vasodilator, nitroprusside, which delivers NO essentially in a burst while simultaneously releasing cyanide.[25,49]

Conclusion

Reduction of *trans*-[RuCl(NO)(cyclam)]$^{2+}$ yields an octahedral {Ru−NO}^{7} system with some localization of the electron on the NO. This results in the fairly rapid loss of chloride followed by the slower loss of NO$^{\bullet}$. Probably owing to its relatively slow dissociation of NO$^{\bullet}$, this complex does not exhibit biological activity either in terms of cancer cell toxicity or in affecting hippocampal neuronal firing. However, it can deliver NO in a controlled manner, acting as a long-lasting, although softer, vasodilator.[25,49] Because of the slow dissociation of NO from *trans*-$[RuCl(NO^{\bullet})(cyclam)]^{2+}$, *trans*-$[RuCl(H_2O)(cyclam)]^{2+}$ and related complexes may prove useful as scavengers of NO in blood.

Acknowledgment. Work at Boston College was supported by NIH GM26390 and CAPES. Research at USP was supported by grants and fellowships from FAPESP, CNPq, and CAPES. We are grateful to the following: Professor Dennis Sardella for help in interpreting ^{1}H NMR data, Dr. Peter Bonitatebus for help with the X-ray data processing, Prof. Alfred Prock (Boston University) for analysis of the square wave kinetic data, and Prof. Bruce McGarvey for assistance with the EPR spectra.

Supporting Information Available: ORTEP diagrams and side views of *trans*-$[Cl(NO)(14ane)Ru]^{2+}$, plot (k_{-NO}/T vs $1/T$) used in the determination of $\Delta H^{\#}$, $\Delta S^{\#}$, $\Delta G^{\#}$, tables of crystal and structure refinement data for *trans*-$[Cl(NO)(14ane)Ru](ClO_4)_2$, atomic coordinates, equivalent isotropic displacement parameters, bond lengths, bond angles, anisotropic displacement parameters, and hydrogen coordinates with isotopic displacement parameters, and additional data in CIF format. This material is available free of charge via the Internet at http://pubs.acs.org.

IC9912979

(44) Armor, J. N.; Hoffman, M. Z. *Inorg. Chem.* **1975**, *14*, 444−446.
(45) Pipes, D. W.; Meyer, T. J. *Inorg. Chem.* **1984**, *23*, 2466−2472.
(46) Lopes, L. G. F.; Castellano, E. E.; Zukerman-Schpector, J.; Ferreira, A. G.; Davanzo, C. U.; Clarke, M. J.; Wieraszko, A.; Franco, D. W. Unpublished results, 2000.
(47) Chen, Y.; Shepherd, R. E. *J. Inorg. Biochem.* **1997**, *68*, 183−193.
(48) Lu, J.; Clarke, M. J. *J. Chem. Soc., Dalton Trans.* **1992**, 1243−1248.
(49) Krieger, M. H.; Souza-Torsoni, A.; Marcondes, F. G.; Franco, D. W.; Toledo, J. C.; Tfouni, E.; Ferro, A. A.; Haun, M.; Sumitami, M. *Hypertension* **1999**, *33*, 159.